Research Paper

Genetic and Pharmacological Inhibition of PAPP-A Reduces Bleomycin-Induced Pulmonary Fibrosis in Aged Mice via Reduced IGF Signaling

Laurie K. Bale,[1] Sally A. West,[1] Claus Oxvig,[2] Kristian S. Andersen,[2] Anja C. Roden,[3]
Andrew J. Haak,[4] and Cheryl A. Conover[1,*]

[1]Department of Endocrinology, Mayo Clinic, Rochester, MN, USA
[2]Department of Molecular Biology and Genetics, Aarhus University, Aarhus, Denmark
[3]Department of Laboratory Medicine and Pathology, Mayo Clinic, Rochester, MN, USA
[4]Department of Physiology and Biomedical Engineering, Mayo Clinic, Rochester, MN, USA
[*]Corresponding author: Conover.Cheryl@mayo.edu
https://doi.org/10.59368/agingbio.20240023

Idiopathic pulmonary fibrosis (IPF) is an age-associated lung disease of unknown etiology that is characterized by exaggerated deposition of extracellular matrix (ECM), leading to distorted lung architecture, respiratory failure, and death. There are no truly effective treatment options for IPF, thus highlighting the importance of exploring new pathogenic mechanisms that underlie the development of fibrosis and of identifying new therapeutic targets. Insulin-like growth factors (IGFs) are known to be pro-fibrotic. However, the ubiquity and essentiality of IGF receptor signaling in normal physiology limit its potential as a direct therapeutic target. In a recent study, we found a highly significant correlation between expression of pregnancy-associated plasma protein (PAPP)-A in human IPF lung tissue and disease severity. PAPP-A is a unique metalloprotease that enhances local IGF action. In vitro studies support a role for proteolytically active PAPP-A in promoting a fibrotic phenotype in adult human lung fibroblasts. Here, we show that PAPP-A is preferentially expressed in mouse lung fibroblasts and that inhibition of PAPP-A in vivo through PAPP-A gene deletion or a specific neutralizing monoclonal antibody against PAPP-A markedly reduced the progression of bleomycin-induced lung fibrosis, as measured by significantly decreased ECM expression and improved lung histology. Surrogate markers of local IGF receptor activity in the lung were also significantly reduced, indicating indirect modulation of IGF signaling through PAPP-A. These results establish a role for PAPP-A in pulmonary fibrosis and point to PAPP-A as a selective and pharmacologically tractable target for IPF and possibly other fibrotic disorders.

Introduction

Pulmonary fibrosis is a component of many interstitial lung diseases, including idiopathic pulmonary fibrosis (IPF). IPF is an irreversible, progressive lung disease of unknown etiology most commonly seen in older adults. This debilitating fibrosis is the result of repetitive alveolar epithelial cell injuries coupled with an unresolved process of wound healing[1,2]. Multiple microsites of ongoing epithelial injury induce the migration and proliferation of fibroblasts and their transformation into myofibroblasts. Myofibroblasts are specialized fibroblasts that exhibit a contractile phenotype, contributing to altered compliance of the lung[3,4]. In fibroblast/myofibroblast foci, there are persistent pro-survival signals and an increased response to fibrogenic factors. This results in exaggerated deposition of extracellular matrix (ECM), leading to irreversibly distorted lung architecture, respiratory failure, and death[5]. There are no truly effective treatment options, and patients with IPF have a median survival of less than three years from diagnosis[1,6–8]. Therefore, it is important to explore new pathogenic mechanisms underlying the development of

fibrosis, and to identify potential therapeutic targets for this deadly disease.

In a recent study, we found a highly significant correlation between pregnancy-associated plasma protein (PAPP)-A expression levels in human IPF lung tissue and disease severity as measured by various pulmonary and physical function tests[9]. These data suggested a newly identified role for PAPP-A in pulmonary fibrosis. PAPP-A is a metalloproteinase that enhances local insulin-like growth factor (IGF) activity through the cleavage of inhibitory IGF-binding proteins, mainly IGFBP-4[10–13]. There are multiple studies linking the IGF system with normal and aberrant wound healing in several tissues, including the lung. IGF-I stimulates proliferation of fibroblasts, protects myofibroblasts from apoptosis, and promotes ECM accumulation—all processes associated with fibrosis of the lung[14–16]. Blockade of IGF-I receptor (IGF-IR) signaling in vivo reduced bleomycin-induced lung injury[17,18]. However, the ubiquity and essentiality of IGF-IR in normal physiology limit its potential as a direct therapeutic target.

In this study, we used an in vivo model of lung injury—bleomycin-induced lung injury in mice—an established model

that produces many, but not all, aspects of human IPF[19–22]. It is widely used in mice to model pulmonary fibrosis for the study of mechanisms involved in fibrogenesis. Herein, we present data comparing the responses of wild-type (WT) and PAPP-A knockout (KO) mice to intratracheal bleomycin administration. Inhibition of PAPP-A expression represents an innovative approach to decreasing IGF availability with moderate restraint of IGF-IR signaling[11]. We have previously shown that inhibition of PAPP-A through gene deletion in mice has many beneficial effects, including a remarkable extension of lifespan by 30%–40% and suppression of atherosclerotic lesion progression[23,24]. Beneficial effects were also seen when administering a monoclonal antibody in vitro and in vivo that specifically inhibits PAPP-A-induced proteolysis of IGFBP-4[9,25–29]. In this study, either PAPP-A gene deletion or pharmacological inhibition of PAPP-A's proteolytic activity against IGFBP-4 significantly reduced bleomycin-induced lung fibrosis in mice via reduced IGF signaling.

Material and Methods

Materials

Bleomycin was purchased from Meitheal Pharmaceuticals (Chicago, IL). A preliminary dose-response study was performed to determine a dose that induced fibrosis but did not result in mortality.

Mice

All procedures were approved by the Institutional Animal Care and Use Committee of the Mayo Clinic.

WT and PAPP-A KO mice were on a mixed C57BL/6 and Sv129/E background. Heterozygous breeding and littermates were used in experiments to minimize the potential impact of different genetic backgrounds. Genotyping was performed at weaning by PCR as described previously[10]. Male and female mice were studied at 4 and 12 to 15 months of age. Genotypes were confirmed with tail-snip DNA collected at the end of the experiment.

Bleomycin-induced lung injury

The standard chow diet was replaced by a breeder diet (PicoLab, St. Louis, MO) starting two weeks prior to surgery in order to increase body weight, and mice were maintained on this diet for the duration of the experiment. Mice were anesthetized with ketamine/xylazine before exposure to the trachea under sterile conditions. Bleomycin (0.7 U/kg) or phosphate-buffered saline (PBS; control) in 50 μl was administered intratracheally while the mouse was hanging on a platform to aid in proper disbursement to the lungs, as previously described[30]. Mice were monitored, weighed, and their body composition score (BCS) recorded daily. Twenty-one days after bleomycin administration, WT and PAPP-A KO mice were euthanized, lungs perfused with PBS to remove any remaining blood, and the left lobe clamped off with a ligation clip (Teleflex Medical, Morrisville, NC) to prevent inflation of this lobe. A small nick was made between the tracheal rings, and a cannula containing 10% buffered formalin was inserted into the trachea. Once the lung was inflated, it was tied off with 5–0 surgical silk. The lungs were then removed and placed in a 50-ml conical tube containing 10% buffered formalin. The left lobe was snap frozen in liquid nitrogen immediately after the inflation of the right lobe. After 48 hours, fixed lung tissues were transferred to 30% sucrose. After five days in sucrose, the lungs were embedded in an optimal cutting temperature (OCT) compound and stored at −80 °C.

In a second strategy, aged WT mice were given weekly intraperitoneal (ip) injections (30 mg/kg) of a specific monoclonal antibody that inhibits PAPP-A's proteolytic activity against IGFBP-4, mAb-PA1/41[25,26], or isotype control (IgG2a, Bio X Cell). mAb-PA1/41 was purified from serum-free culture medium using a HiTrap Protein G column (Cytiva). The bound antibody was eluted with 0.1 M glycine, pH 2.2, followed by immediate neutralization with 1M Tris, pH 9. Further purification and buffer exchange were performed on a Superdex TM 200 increase 10/300 GL column (Cytiva), equilibrated with endotoxin-free PBS (137 mM NaCl, 10 mM Na_2HPO_4, 1.8 mM KH_2PO_4, and 2.7 mM KCl at pH 7.4). Treatment was started seven days after bleomycin administration, and lungs were harvested as above at day 21.

Weight loss approaching 30% of the initial weight, a BCS of 1, and/or signs of lethargy were clinical criteria for the euthanasia of the mouse and the removal of their data from the study. Only two male mice (1 WT, 1 KO) out of over 70 bleomycin-treated mice in these studies reached the criteria for euthanasia before the day 21 endpoint. No PBS-treated control mice were lost.

Fluorescence-activated cell sorting

Lungs from sham or bleomycin-treated mice were enzymatically digested for markers of epithelial cells, endothelial cells, and fibroblasts, followed by RNA isolation and quantitative real-time PCR (RT-qPCR) as previously described[30].

RT-qPCR

Total RNA was isolated from the pulverized left lobe of the lung, lyzed with 1 ml of Trizol (Ambion Life Technologies, Carlsbad, CA), and further processed as per the manufacturer's instruction. It was then reverse transcribed with the SuperScript III First-Strand Synthesis System (Life Technologies) and evaluated by RT-qPCR using the CFX Connect Real-Time System with iTAQ Universal SYBR Green Supermix (Bio-Rad, Hercules, CA). Amplification plots were analyzed using CFX Maestro Software version 4.1 (Bio-Rad). To create standard curves, designed primers were PCR'd with cDNA from normal mouse tibia and quadriceps. Amplified PCR products were purified through the QIAquick Gel Extraction Kit (Qiagen Hilden, Germany), quantified, and serially diluted from 10^8 to 10^3 molecules. Relative quantification and fold changes were based on the standard curve for each gene. Primers used for mouse collagen (COL1a1, COL3a1), fibronectin (FN), IGFBP-5, GAPDH, and TBP are listed in **Table 1**.

Western blot

Lung tissue was pulverized under liquid nitrogen temperatures, and the powder was immediately placed in RIPA buffer with protease (complete mini tablet, Roche Diagnostics) and phosphatase inhibitors (2 mM sodium orthovanadate, 10 mM sodium pyrophosphate, 40 mM beta-glycerolphosphate, and 10 mM sodium fluoride). Samples were homogenized with a motorized tissue grinder and pestle and sonicated for five seconds before centrifuging to obtain supernatant, all at 4 °C. Samples were loaded on 7.5% TGX mini gels (BioRad), transferred to polyvinyl difluoride filters membranes, blocked with 3% BSA/TBS-T, and placed in primary antibody overnight at 4'C. Phosphorylated Akt (S473) and total Akt (Cell Signaling Technology) were used at a 1:1000 dilution. Blots were washed with TBS-T, incubated with goat anti-rabbit HRP conjugated secondary antibody at a

Table 1. Primers for quantitative real-time PCR.

Mus musculus collagen, type I, alpha 1 (m.Col1a1), NM_007742.4
Forward: cgatggattcccgttcgagt
Reverse: cgatctcgttggatccctgg
197 bp
Mus musculus collagen, type III, alpha 1 (Col3a1)
Forward: acgtagatgaattgggatgcag
Reverse: gggttggggcagtctagtg
154 bp
Mus musculus fibronectin 1 (Fn1), transcript variant X1 (m.EDA-FM), XM_006495697.4
Forward: gaaggtttgcaacccactgt
Reverse: catcctcagggctcgagtag
217 bp
Mus musculus insulin-like growth factor binding protein 5 (Igfbp5), NM_010518.2
Forward: gaacactgcccaccccagag
Reverse: ccacgggagggcttacactg
195 bp
Mus musculus glyceraldehyde-3-phosphate dehydrogenase (m.Gapdh), NM_008084.2
Forward: ttcaccaccatggagaagg
Reverse: ctcgtggttcacacccatc
111 bp
Mus musculus TATA box binding protein (m.TBP), NM_013684.3
Forward: ctcagttacaggtggcagca
Reverse: cagcacagagcaagcaactc
120 bp

1:5000 dilution (Jackson ImmunoResearch Laboratories, Inc.) for one hour at room temperature, washed again, exposed to ECL blotting substrate (Pierce/thermo scientific), imaged on an Odyssey Fc imaging system, and bands quantified using Empiria Studio Software (LI-COR).

Histology

OCT-embedded right lung lobes were sectioned to a thickness of 8 um using an Epredia cryostat (model # HM525 NX) at −26 °C. Slides were stained for H&E and Masson's trichome using reagents from Millipore-Sigma (St. Louis, MO) following the manufacturer's instructions. Analysis of the morphology and histology was performed by a board-certified thoracic pathologist (A.C.R.) who was blinded to the samples. Quantitation employed an established scoring system to evaluate the extent of fibrosis and staining in all four lobes[31]. All stained slides were systematically scanned at 100× magnification, and successive 100× fields were scored. Scoring was based on the following scales: 0 (no fibrosis), 1 (minimal interstitial and/or peribronchiolar thickening due to fibrosis), 3 (moderate thickening without obvious architectural distortion), 5 (increased fibrosis with the formation of fibrous bands and/or small masses), and 7 (severe architectural distortion with large areas of fibrosis with or without honeycomb changes). The predominant score for each field was recorded. The median score for all fields (25–35 fields per lung) was calculated for each mouse.

Statistical analyses

Indicators of statistical significance were the unpaired Student's t-test and the Mann–Whiney nonparametric test, with significance set at $p < 0.05$.

Results

PAPP-A expression in mouse lung cells

In a preliminary study, fluorescent-activated cell-sorted fibroblasts, epithelial cells, and endothelial cells were isolated from the lung of mice following bleomycin administration[30]. PAPP-A was highly expressed in lung-derived fibroblasts, and this expression was increased approximately threefold with bleomycin treatment. In comparison, there was little PAPP-A expressed in lung-derived epithelial and endothelial cells even after bleomycin treatment (Fig. 1). Thus, the data indicate that fibroblasts, considered the prime effectors of tissue scarring, are the main cell type expressing PAPP-A in the mouse lung, and this expression is increased with bleomycin-induced lung injury. We therefore determined how the loss of PAPP-A expression or proteolytic activity would influence lung fibrosis.

Effect of PAPP-A gene deletion in the response to bleomycin-induced lung fibrosis

In an initial study, young (four-month-old) WT and PAPP-A KO male and female mice were administered bleomycin or PBS intratracheally. Lungs were evaluated 21 days after bleomycin (Table 2), as detailed in the Material and Methods section. Expression levels of type I collagen (COL1a1) and FN showed considerable variation, and the only significant effect of PAPP-A gene deletion on the bleomycin response in these young mice was with female FN. IPF predominantly affects middle-aged and elderly adults, suggesting a mechanistic link between chronological age and this disease. Aging is the driving force of IPF, and bleomycin injury causes worse lung fibrosis in old mice than in young mice[32]. Furthermore, the use of aged mice more closely models IPF in humans and is recommended by the Office of the American Thoracic Society Workshop Report on the use of animal models for preclinical assessment of potential therapies for
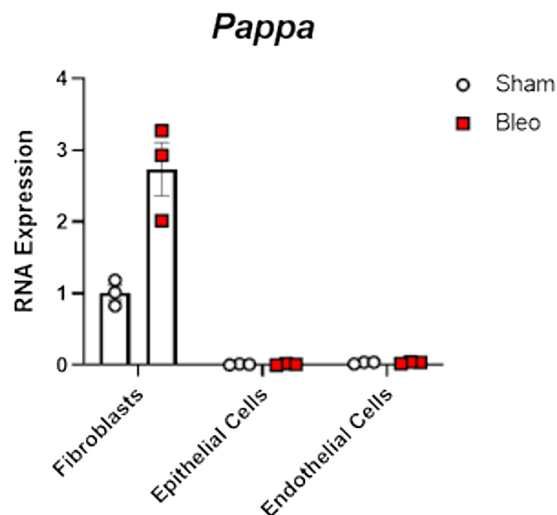

Figure 1. Pregnancy-associated plasma protein (PAPP)-A expression in presorted cell types from the lungs of mice without (sham) or with bleomycin administration.

Table 2. Relative mRNA expression in lungs from young wild-type (WT) and pregnancy-associated plasma protein (PAPP)-A knockout (KO) mice.

	WT	PAPP-A KO	p-Value
Males			
COL1a1	1.1 ± 0.34	0.6 ± 0.28	0.32
FN	2.9 ± 0.32	2.0 ± 0.32	0.08
Females			
COL1a1	1.1 ± 0.14	0.8 ± 0.23	0.09
FN	1.2 ± 0.14	0.6 ± 0.10	0.006

FN, fibronectin.

Results are relative expression, mean $\pm$ SEM, n = 7–11.

Day 21 after bleomycin administration, lungs from 4-month-old WT and PAPP-A KO mice were harvested and processed by quantitative real-time PCR for mRNA analyses.

GAPDH was used as an internal reference control. Similar results were obtained using TBP.

pulmonary fibrosis[22]. Thus, in the next studies, we used both male and female mice at 12 to 15 months of age.

Bleomycin treatment had marked effects on the expression of ECM components (**Table 3**; PBS vs. bleomycin), with significant increases in COL1a1, COL3a1, and FN mRNA in the lungs of male and female mice. **Table 4** presents relative changes in WT versus PAPP-A KO lungs with bleomycin treatment. There were significant reductions in COL1a1 and COL3a1 expression (20%–50%) in male and female PAPP-A KO mice compared to WT mice in response to bleomycin. FN expression was significantly reduced by 44% in male PAPP-A KO mice. The 22% reduction in FN expression in female PAPP-A KO mice did not reach statistical significance. Thus, molecular analyses suggest decreased expression of major ECM components in PAPP-A KO mouse lungs in response to injury. However, our numbers were insufficient to determine any difference in baseline gene expression between WT and PAPP-A KO mice.

IGFBP-5, an IGF-responsive gene, was used as a surrogate marker for IGF activity in vivo (**Table 4**). IGFBP-5 mRNA levels were significantly reduced in the lung in both male (38%) and female (27%) PAPP-A KO mice compared to WT after bleomycin administration. This fits with the concept that loss of PAPP-A reduces local IGF-IR signaling, as shown in other studies[24,33–37]. The level of pAKT, another marker of IGF-IR activity through

Table 3. Relative mRNA expression of extracellular matrix components in mouse lung—phosphate-buffered saline (PBS) versus bleomycin treatment in wild-type mice.

	PBS	Bleomycin	p-Value
Males			
COL1a1	0.09 ± 0.007	0.63 ± 0.071	<0.0001
COL3a1	0.05 ± 0.005	0.20 ± 0.02	<0.0001
FN	0.04 ± 0.007	0.39 ± 0.038	<0.0001
Females			
COL1a1	0.05 ± 0.061	1.68 ± 0.269	0.0004
COL3a1	0.07 ± 0.016	0.59 ± 0.033	<0.0001
FN	0.04 ± 0.008	1.00 ± 0.207	0.0007

FN, fibronectin.

Results are relative expression, mean $\pm$ SEM, n = 6–13 per treatment group.

Table 4. Relative mRNA expression in lungs from old wild-type (WT) and pregnancy-associated plasma protein (PAPP)-A knockout (KO) mice.

	WT	PAPP-A KO (%)	p-Value
Males			
COL1a1	100 ± 11	57 ± 7	0.006
COL3a1	100 ± 2	50 ± 5	0.004
FN	100 ± 10	56 ± 7	0.007
IGFBP-5	100 ± 12	62 ± 9	0.022
Females			
COL1a1	100 ± 8	68 ± 7	0.009
COL3a1	100 ± 2	48 ± 8	0.008
FN	100 ± 10	78 ± 12	0.210
IGFBP-5	100 ± 8	73 ± 5	0.016

FN, fibronectin.

Results (mean $\pm$ SEM, n = 8–12) are presented as % of WT value set at 100.

Day 21 after bleomycin administration, lungs from 12- to 15-month-old WT and PAPP-A KO mice were harvested and processed by quantitative real-time PCR for mRNA analyses.

GAPDH was used as an internal reference control. Similar results were obtained using TBP.

the phosphatidylinositol 3-kinase pathway[5,15], was reduced by $44 \pm 10\%$ (n = 4) in the lungs of PAPP-A KO mice compared to WT mice. A representative Western blot is presented in **Figure 2**.

Lung fibrosis and architecture of WT and PAPP-A KO mice were assessed on histological sections using an Ashcroft scoring system[31]. Representative Masson trichrome-stained sections are shown in **Figure 3**, and calculated scores are shown in **Figure 4**. Normal untreated lungs and lungs administered PBS at surgery scored 0 (no fibrosis). Lungs of male WT mice 21 days after bleomycin scored 4.6 ± 0.60 with many confluent fibrotic masses, abundant collagen fibrils (blue staining), and damaged lung structure. Male PAPP-A KO mice 21 days after bleomycin scored 1.7 ± 0.84 with minimal interstitial thickening due to fibrosis without obvious architectural distortion. This 60% reduction of fibrosis in male PAPP-A KO mice was highly significant (p = 0.02). Similar reductions in fibrosis, ~40% (p = 0.02), were seen in female PAPP-A KO mice (**Fig. 4**).

Effect of pharmacological inhibition of PAPP-A activity in the response to bleomycin-induced lung fibrosis

Inflammation is not a driving component in human IPF, but it is an early phase of bleomycin-induced lung injury models, which resolves in about seven days[38,39]. It is recommended that the efficacy of therapies in the bleomycin model is best determined after the inflammatory phase[40,41]. To limit the potential impact of this phase on fibrosis and to take a more translational approach, we administered bleomycin intratracheally to aged male and female WT mice and then waited seven days before ip administration of a monoclonal antibody inhibitor of PAPP-A's proteolytic activity against IGFBP-4 (mAb-PA1/41) or IgG2 isotype as a control. Injections were repeated the following week, and lungs were harvested 21 days after bleomycin administration. As shown in **Table 5**, COL1a1 and COL3a1 expression were significantly reduced by 30%–60% with mAb-PA1/41 treatment in both male and female mice. FN and IGFBP-5 mRNA expression were also reduced with mAb-PA1/41 treatment (~60% and ~30%,

Figure 2. Representative Western blot of phosphorylated and total Akt in the lungs of wild-type (WT) and PAPP-A knockout (KO) mice and in the lungs of IgG- and mAb-PA1/41-treated mice.

Figure 3. Masson's trichrome staining of mouse lungs. Representative images of fibrosis in the lungs of aged WT and PAPP-A KO mice 21 days after bleomycin or phosphate-buffered saline (control) administration. Ashcroft scores for each image are indicated in parentheses: 0 (no fibrosis), 3 (moderate thickening without obvious architectural distortion), 5 (increased fibrosis with the formation of fibrous bands with large areas of fibrosis), and 7 (severe architectural distortion with large areas of fibrosis). White arrow indicates a mass of newly formed collagen fibrils. 5× magnification.

Figure 4. Ashcroft score of stained lung sections from aged WT and PAPP-A KO mice 21 days after bleomycin administration. Each filled circle is a value for an individual mouse. *$P = 0.02$, Mann–Whitney test.

Table 5. Relative mRNA expression in lungs from old wild-type (WT) mice treated with pregnancy-associated plasma protein-A neutralizing mAb or isotype control (IgG).

	IgG	mAb (%)	p-Value
Males			
COL1a1	100 ± 11	63 ± 9	0.030
COL3a1	100 ± 2	31 ± 3	0.002
FN	100 ± 35	37 ± 8	0.047
IGFBP-5	100 ± 10	67 ± 5	0.013
Females			
COL1a1	100 ± 12	47 ± 10	0.007
COL3a1	100 ± 2	27 ± 3	0.002
FN	100 ± 45	41 ± 9	0.097
IGFBP-5	100 ± 10	70 ± 10	0.052

FN, fibronectin.
Results (mean $\pm$ SEM, n = 5–7) are presented as % of IgG value set at 100. Weekly injections of mAb-PA1/41 or IgG were started seven days after bleomycin administration to 12- to 15-month-old WT mice, and lungs harvested 21 days after bleomycin treatment and processed by quantitative real-time PCR for mRNA analyses.
GAPDH was used as an internal reference control. Similar results were obtained using TBP.
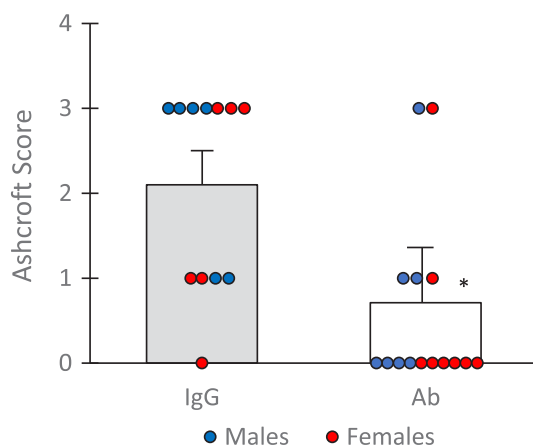
Figure 5. Ashcroft score of stained lung sections from WT mice treated with PAPP-A neutralizing antibody (mAb-PA1/41) or IgG control started seven days after bleomycin administration and was harvested at day 21. Blue-filled circles are males; red-filled circles are females. $*P = 0.009$, Mann–Whitney test.

respectively). Bleomycin-induced lung fibrosis (Ashcroft score) was significantly reduced by ~70% with mAb-PA1/41 treatment (Fig. 5). IGF signaling, as assessed by pAkt, was reduced by $60\% \pm 20\%$ (n = 4) in the lungs of mAb-PA1/41-treated mice compared to IgG-treated mice (see, e.g., Fig. 2).

Discussion

IPF is an irreversible, progressive lung disease most commonly seen in older adults. At present, there are no truly effective treatment options for this deadly disease. A better understanding of the mechanisms underlying the development of fibrosis has the potential to lead to new therapeutic targets. Our studies present

molecular, biochemical, and histological evidence that genetic or pharmacological inhibition of PAPP-A reduces bleomycin-induced lung fibrosis in aged male and female mice.

We saw little bleomycin-induced ECM changes in young mice, even though many such studies have been done in mice 4–8 weeks old. This could be due to the use of different background strains, dosage of bleomycin, and animal size[22]. It is clear from our and others' data that bleomycin injury produces worse lung fibrosis in old mice than in young mice, and it has been suggested that aged lungs manifest a pro-fibrotic phenotype with increased COL1a1 and FN expression that is more susceptible to injury[42].

Thus, we compared the fibrotic response in aged WT and PAPP-A KO mice 21 days after intratracheal administration of bleomycin. There was significantly reduced expression of type I collagen and FN mRNA in the lungs of PAPP-A KO mice compared to WT mice. Histological grading of lung sections and visual identification of collagen fibrils by Masson's trichrome staining confirmed these findings. It is of note that PAPP-A KO mice are born as proportional dwarfs and retain this phenotype through life[10]. They are long-lived, but dwarfism *per se* does not result in a longevity phenotype, since normal-sized PAPP-A KO mice retain a longevity phenotype[43,44]. Aging is a strong risk factor for developing IPF[45], and both are associated with the accumulation of senescent cells in the lung[40,46,47]. PAPP-A/IGF-I signaling is also associated with aging[23] and senescence in the lung[9,30]. In this study, PAPP-A KO mice and mice treated with PAPP-A inhibitory antibody had reduced markers of IGF activity, that is, IGFBP-5 gene expression and PI3K/Akt signaling. Thus, PAPP-A is associated with major "hallmarks of aging": intercellular communication through IGF signaling and cellular senescence[48]. However, cellular senescence could not be established in this study using whole lung tissue (data not shown), as could be shown in isolated lung fibroblasts[9,40,46,47].

Although the use of genetically modified mice in the first study may be suitable for discovery research, that is, the novel finding that PAPP-A gene deletion reduces the fibrotic response in aged mice, another approach using normal adult mice for preclinical application of experimental findings is necessary. Therefore, the second set of studies in aged WT male and female mice used a weekly ip injection of an IgG isotype or a specific inhibitor of PAPP-A-mediated IGFBP-4 proteolysis (mAb-PA1/41), which has been shown to be effective in other studies[25–29]. This inhibitor of PAPP-A action was started seven days after intratracheal bleomycin to distinguish between the effects of inflammation and active fibrosis progression[41]. The results at 21 days were similar to PAPP-A gene deletion, with a significant reduction in ECM expression and delayed development of lung fibrosis, suggesting that inflammation is not a major contributor to the beneficial effect of PAPP-A inhibition in this model. Indeed, pro-inflammatory cytokines are known to increase PAPP-A expression and not vice versa[49,50]. Likewise, Huang et al.[51] found that transgenic overexpression of a natural inhibitor of PAPP-A, stanniocalcin-1[52], protected against bleomycin-induced lung fibrosis. However, further studies should look at inflammatory markers in chronic fibrotic disease.

IGFBP-5 is an IGF-responsive gene used as an in vivo surrogate for IGF-IR-mediated action[33–37]. We found decreased IGFBP-5 mRNA in PAPP-A KO versus WT lungs and in Ab-PA1/41-treated mice versus control, indicating decreased IGF signaling. Also, the PI3K/Akt anti-apoptotic pathway[5] was suppressed in PAPP-A KO lungs. In Choi et al.[17], blocking IGF-IR activation

increased apoptosis, limited fibroblast migration, and reduced bleomycin-induced fibrosis in mice. We speculate similar mechanisms are in play when the enhancing effect of PAPP-A on IGF signaling is inhibited.

In conclusion, we have demonstrated that inhibition of PAPP-A in adult mice has an anti-fibrotic effect in vivo. Therefore, selective inhibition of this enzyme with a neutralizing monoclonal antibody, such as mAb-PA1/41, is a promising therapeutic approach for IPF and perhaps other fibrotic diseases.

Acknowledgments

Funding

Author Contributions

C.A.C. and A.J.H. conceived and designed the experiments. L.K.B. and S.A.W. performed the experiments. A.C.R. did the histological scoring. C.O. and K.S.A. produced, purified, and tested the PAPP-A inhibitory antibody used in the study. C.A.C. prepared figures and drafted the article. All authors reviewed the article and approved the final version.

References

1. Vancheri C., Failla M., Crimi N., & Raghu G. (2010). Idiopathic pulmonary fibrosis: A disease with similarities and links to cancer biology. *Eur. Respir. J.* **35**(3), 496–504. PMID: 20190329; doi: 10.1183/09031936.00077309.

2. Venosa A. (2020). Senescence in pulmonary fibrosis: Between aging and exposure. *Front Med.* **7**. PMID: 33282895; doi: 10.3389/fmed.2020.606462.

3. Phan S.H. (2002). The myofibroblast in pulmonary fibrosis. *Chest* **122**(6), 286S–289S. PMID: 12475801; doi: 10.1378/chest.122.6_suppl.286S.

4. Scotton C.J., & Chambers R.C. (2007). Molecular targets in pulmonary fibrosis: The myofibroblast in focus. *Chest* **132**(4), 1311–1321. PMID: 17934117; doi: 10.1378/chest.06-2568.

5. Thannickal V.J., & Horowitz J.C. (2006). Evolving concepts of apoptosis in idiopathic pulmonary fibrosis. *Proc. Am. Thorac. Soc.* **3**(4), 350–356. PMID: 16738200; doi: 10.1513/pats.200601-001TK.

6. Raghu G., Collard H.R., Egan J.J., Martinez F.J., Behr J., Brown K.K., … Schünemann H.J. (2011). An official ATS/ERS/JRS/ALAT statement: Idiopathic pulmonary fibrosis: Evidence-based guidelines for diagnosis and management. *Am. J. Respir. Crit. Care Med.* **183**(6), 788–824. PMID: 21471066; doi: 10.1164/rccm.2009-040GL.

7. Barratt S.L., Creamer A., Hayton C., & Chaudhuri N. (2018). Idiopathic pulmonary fibrosis (IPF): An overview. *J. Clin. Med.* **7**(8). PMID: 30082599; doi: 10.3390/jcm7080201.

8. Suri G.S., Kaur G., Jha C.K., & Tiwari M. (2021). Understanding idiopathic pulmonary fibrosis - Clinical features, molecular mechanism and therapies. *Exp. Gerontol.* **153**, 111473. PMID: 34274426; doi: 10.1016/j.exger.2021.111473.

9. Bale L.K., Schafer M.J., Atkinson E.J., Le Brasseur N.K., Haak A.J., Oxvig C., & Conover C.A. (2022). Pregnancy-associated plasma protein-A (PAPP-A) is a key component of an interactive cellular mechanism promoting pulmonary fibrosis. *J. Cell Physiol.* **237**(4), 2220–2229. PMID: 35098542; doi: 10.1002/jcp.30687.

10. Conover C.A., Bale L.K., Overgaard M.T., Johnstone E.W., Laursen U.H., Füchtbauer E.M., … van Deursen J. (2004). Metalloproteinase pregnancy-associated plasma protein A is a critical growth regulatory factor during fetal development. *Development* **131**(5), 1187–1194. PMID: 14973274; doi: 10.1242/dev.00997.

11. Conover C.A. (2012). Key questions and answers about pregnancy-associated plasma protein-A. *Trends Endocrinol. Metab.* **23**(5), 242–249. PMID: 22463950; doi: 10.1016/j.tem.2012.02.008.

12. Laursen L.S., Overgaard M.T., Weyer K., Boldt H.B., Ebbesen P., Christiansen M., … Oxvig C. (2002). Cell surface targeting of pregnancy-associated plasma protein A proteolytic activity. Reversible adhesion is mediated by two neighboring short consensus repeats. *J. Biol. Chem.* **277**(49), 47225–47234. PMID: 12370176; doi: 10.1074/jbc.M209155200.

13. Conover C.A., & Oxvig C. (2023). The pregnancy-associated plasma protein-A (PAPP-A) story. *Endocr. Rev.* PMID: 37267421; doi: 10.1210/endrev/bnad017.

14. Hung C.F., Rohani M.G., Lee S.S., Chen P., & Schnapp L.M. (2013). Role of IGF-1 pathway in lung fibroblast activation. *Respir. Res.* **14**(1), 102. PMID: 24103846; doi: 10.1186/1465-9921-14-102.

15. Kooijman R. (2006). Regulation of apoptosis by insulin-like growth factor (IGF)-I. *Cytokine Growth Factor Rev.* **17**(4), 305–323. PMID: 16621671; doi: 10.1016/j.cytogfr.2006.02.002.

16. Kurmasheva R.T., & Houghton P.J. (2006). IGF-I mediated survival pathways in normal and malignant cells. *Biochim. Biophys. Acta* **1766**(1), 1–22. PMID: 16844299; doi: 10.1016/j.bbcan.2006.05.003.

17. Choi J.E., Lee S.S., Sunde D.A., Huizar I., Haugk K.L., Thannickal V.J., … Schnapp L.M. (2009). Insulin-like growth factor-I receptor blockade improves outcome in mouse model of lung injury. *Am. J. Respir. Crit. Care Med.* **179**(3), 212–219. PMID: 19011156; doi: 10.1164/rccm.200802-228OC.

18. Hernandez D.M., Kang J.H., Choudhury M., Andrianifahanana M., Yin X., Limper A.H., & Leof E.B. (2020). IPF pathogenesis is dependent upon TGFbeta induction of IGF-1. *FASEB J.* **34**(4), 5363–5388. PMID: 32067272; doi: 10.1096/fj.201901719RR.

19. Peng R., Sridhar S., Tyagi G., Phillips J.E., Garrido R., Harris P., … Stevenson C.S. (2013). Bleomycin induces molecular changes directly relevant to idiopathic pulmonary fibrosis: A model for "active" disease. *PLoS One* **8**(4), e59348. PMID: 23565148; doi: 10.1371/journal.pone.0059348.

20. Walters D.M., & Kleeberger S.R. (2008). Mouse models of bleomycin-induced pulmonary fibrosis. *Curr. Protoc. Pharmacol.* **Chapter 5**, Unit 5.46. PMID: 22294226; doi: 10.1002/0471141755.ph0546s40.

21. Ruscitti F., Ravanetti F., Bertani V., Ragionieri L., Mecozzi L., Sverzellati N., … Stellari F.F. (2020). Quantification of lung fibrosis in IPF-like mouse model and pharmacological response to treatment by micro-computed tomography. *Front Pharmacol.* **11**, 1117. PMID: 32792953; doi: 10.3389/fphar.2020.01117.

22. Jenkins R.G., Moore B.B., Chambers R.C., Eickelberg O., Königshoff M., Kolb M., … White E.S. (2017). An Official American Thoracic Society Workshop Report: Use of animal models for the preclinical assessment of potential therapies for pulmonary fibrosis. *Am. J. Respir. Cell Mol. Biol.* **56**(5), 667–679. PMID: 28459387; doi: 10.1165/rcmb.2017-0096ST.

23. Conover C.A., Bale L.K., Mader J.R., Mason M.A., Keenan K.P., & Marler R.J. (2010). Longevity and age-related pathology of mice deficient in pregnancy-associated plasma protein-A. *J. Gerontol. A Biol. Sci. Med. Sci.* **65**(6), 590–599. PMID: 20351075; doi: 10.1093/gerona/glq032.

24. Harrington S.C., Simari R.D., & Conover C.A. (2007). Genetic deletion of pregnancy-associated plasma protein-A is associated with resistance to atherosclerotic lesion development in apolipoprotein E-deficient mice challenged with a high-fat diet. *Circ. Res.* **100**(12), 1696–1702. PMID: 17510462; doi: 10.1161/CIRCRESAHA.106.146183.

25. Mikkelsen J.H., Gyrup C., Kristensen P., Overgaard M.T., Poulsen C.B., Laursen L.S., & Oxvig C. (2008). Inhibition of the proteolytic activity of pregnancy-associated plasma protein-A by targeting substrate exosite binding. *J. Biol. Chem.* **283**(24), 16772–16780. PMID: 18434323; doi: 10.1074/jbc.M802429200.

26. Mikkelsen J.H., Resch Z.T., Kalra B., Savjani G., Kumar A., Conover C.A., & Oxvig C. (2014). Indirect targeting of IGF receptor signaling in vivo by substrate-selective inhibition of PAPP-A proteolytic activity. *Oncotarget.* **5**(4), 1014–1025. PMID: 24572990; doi: 10.18632/oncotarget.1629.

27. Conover C.A., Bale L.K., & Oxvig C. (2016). Targeted inhibition of pregnancy-associated plasma protein-A activity reduces atherosclerotic plaque burden in mice. *J. Cardiovasc. Transl. Res.* **9**(1), 77–79. PMID: 26733326; doi: 10.1007/s12265-015-9666-9.

28. Ramakrishna A., Bale L.K., West S.A., & Conover C.A. (2020). Genetic and pharmacological inhibition of PAPP-A protects against visceral obesity in mice. *Endocrinology* **161**(10). PMID: 32888014; doi: 10.1210/endocr/bqaa160.

29. Becker M.A., Haluska P. Jr, Bale L.K., Oxvig C., & Conover C.A. (2015). A novel neutralizing antibody targeting pregnancy-associated plasma protein-a inhibits ovarian cancer growth and ascites accumulation in patient mouse tumorgrafts. *Mol. Cancer Ther.* **14**(4), 973–981. PMID: 25695953; doi: 10.1158/1535-7163.MCT-14-0880.

30. Schafer M.J., White T.A., Iijima K., Haak A.J., Ligresti G., Atkinson E.J., … LeBrasseur N.K. (2017). Cellular senescence mediates fibrotic pulmonary disease. *Nat. Commun.* **8**(1), 14532. PMID: 28230051; doi: 10.1038/ncomms14532.

31. Ashcroft T., Simpson J.M., & Timbrell V. (1988). Simple method of estimating severity of pulmonary fibrosis on a numerical scale. *J. Clin. Pathol.* **41**(4), 467–470. PMID: 3366935; doi: 10.1136/jcp.41.4.467.

32. Redente E.F., Jacobsen K.M., Solomon J.J., Lara A.R., Faubel S., Keith R.C., … Riches D.W. (2011). Age and sex dimorphisms contribute to the severity of bleomycin-induced lung injury and fibrosis. *Am. J. Physiol. Lung Cell Mol. Physiol.* **301**(4), L510–L518. PMID: 21743030; doi: 10.1152/ajplung.00122.2011.

33. Mohrin M., Liu J., Zavala-Solorio J., Bhargava S., Maxwell Trumble J., Brito A., … Freund A. (2021). Inhibition of longevity regulator PAPP-A modulates tissue homeostasis via restraint of mesenchymal stromal cells. *Aging Cell* **20**(3), e13313. PMID: 33561324; doi: 10.1111/acel.13313.

34. Resch Z.T., Simari R.D., & Conover C.A. (2006). Targeted disruption of the pregnancy-associated plasma protein-A gene is associated with diminished smooth muscle cell response to insulin-like growth factor-I and resistance to neointimal hyperplasia after vascular injury. *Endocrinology* **147**(12), 5634–5640. PMID: 16959843; doi: 10.1210/en.2006-0493.

35. Swindell W.R., Masternak M.M., & Bartke A. (2010). In vivo analysis of gene expression in long-lived mice lacking the pregnancy-associated plasma protein A (PappA) gene. *Exp. Gerontol.* **45**(5), 366–374. PMID: 20197085; doi: 10.1016/j.exger.2010.02.009.

36. Ye P., & D'Ercole J. (1998). Insulin-like growth factor I (IGF-I) regulates IGF binding protein-5 gene expression in the brain. *Endocrinology* **139**(1), 65–71. PMID: 9421399; doi: 10.1210/endo.139.1.5676.

37. Duan C., Liimatta M.B., & Bottum O.L. (1999). Insulin-like growth factor (IGF)-I regulates IGF-binding protein-5 gene expression through the phosphatidylinositol 3-kinase, protein kinase B/Akt, and p70 S6 kinase signaling pathway. *J. Biol. Chem.* **274**(52), 37147–37153. PMID: 10601276; doi: 10.1074/jbc.274.52.37147.

38. Izbicki G., Segel M.J., Christensen T.G., Conner M.W., & Breuer R. (2002). Time course of bleomycin-induced lung fibrosis. *Int. J. Exp. Pathol.* **83**(3), 111–119. PMID: 12383190; doi: 10.1046/j.1365-2613.2002.00220.x.

39. Schiller H.B., Fernandez I.E. , Burgstaller G., Schaab C., Scheltema R.A., Schwarzmayr T., … Mann M. (2015). Time- and compartment-resolved proteome profiling of the extracellular niche in lung injury and repair. *Mol. Syst. Biol.* **11**(7), 819. PMID: 26174933; doi: 10.15252/msb.20156123.

40. Hohmann M.S., Habiel D.M., Coelho A.L., Verri W.A. Jr, & Hogaboam C.M. (2019). Quercetin enhances ligand-induced apoptosis in senescent idiopathic pulmonary fibrosis fibroblasts and reduces lung fibrosis in vivo. *Am. J. Respir. Cell Mol. Biol.* **60**(1), 28–40. PMID: 30109946; doi: 10.1165/rcmb.2017-0289OC.

41. Scotton C.J., & Chambers R.C. (2010). Bleomycin revisited: Towards a more representative model of IPF? *Am. J. Physiol. Lung Cell Mol. Physiol.* **299**(4), L439–L441. PMID: 20675435; doi: 10.1152/ajplung.00258.2010.

42. Sueblinvong V., Neujahr D.C., Mills S.T., Roser-Page S., Ritzenthaler J.D., Guidot D., … Roman J. (2012). Predisposition for disrepair in the aged lung. *Am. J. Med. Sci.* **344**(1), 41–51. PMID: 22173045; doi: 10.1097/MAJ.0b013e318234c132.

43. Bale L.K., & Conover C.A. (2005). Disruption of insulin-like growth factor-II imprinting during embryonic development rescues the dwarf phenotype of mice null for pregnancy-associated plasma protein-A. *J. Endocrinol.* **186**(2), 325–331. PMID: 16079258; doi: 10.1677/joe.1.06259.

44. Bale L.K., West S.A., & Conover C.A. (2017). Inducible knockdown of pregnancy-associated plasma protein-A gene expression in adult female mice extends life span. *Aging Cell* **16**(4), 895–897. PMID: 28600811; doi: 10.1111/acel.12624.

45. Pardo A., & Selman M. (2016). Lung fibroblasts, aging, and idiopathic pulmonary fibrosis. *Ann. Am. Thorac. Soc.* **13**(Suppl 5), S417–S421. PMID: 28005427; doi: 10.1513/AnnalsATS.201605-341AW.

46. Alvarez D., Cárdenes N., Sellarés J., Bueno M., Corey C., Hanumanthu V.S., … Rojas M. (2017). IPF lung fibroblasts have a senescent phenotype. *Am. J. Physiol. Lung Cell Mol. Physiol.* **313**(6), L1164–L1173. PMID: 28860144; doi: 10.1152/ajplung.00220.2017.

47. Morty R.E., & Prakash Y.S. (2019). Senescence in the lung: Is this getting old? *Am. J. Physiol. Lung Cell Mol. Physiol.* **316**(5), L822–L825. PMID: 30892079; doi: 10.1152/ajplung.00081.2019.

48. Lopez-Otin C., Blasco M.A., Partridge L., Serrano M., & Kroemer G. (2013). The hallmarks of aging. *Cell* **153**(6), 1194–1217. PMID: 23746838; doi: 10.1016/j.cell.2013.05.039.

49. Resch Z.T., Chen B.K., Bale L.K., Oxvig C., Overgaard M.T., & Conover C.A. (2004). Pregnancy-associated plasma protein a gene expression as a target of inflammatory cytokines. *Endocrinology* **145**(3), 1124–1129. PMID: 14657012; doi: 10.1210/en.2003-1313.

50. Resch Z.T., Oxvig C., Bale L.K., & Conover C.A. (2006). Stress-activated signaling pathways mediate the stimulation of pregnancy-associated plasma protein-A expression in cultured human fibroblasts. *Endocrinology* **147**(2), 885–890. PMID: 16269458; doi: 10.1210/en.2005-0908.

51. Huang L., Zhang L., Ju H., Li Q., Pan J.S., Al-Lawati Z., & Sheikh-Hamad D. (2015). Stanniocalcin-1 inhibits thrombin-induced signaling and protects from bleomycin-induced lung injury. *Sci. Rep.* **5**, 18117. PMID: 26640170; doi: 10.1038/srep18117.

52. Kloverpris S., Mikkelsen J.H., Pedersen J.H., Jepsen M.R., Laursen L.S., Petersen S.V., & Oxvig C. (2015). Stanniocalcin-1 potently inhibits the proteolytic activity of the metalloproteinase pregnancy-associated plasma protein-A. *J. Biol. Chem.* **290**(36), 21915–21924. PMID: 26195635; doi: 10.1074/jbc.M115.650143.